

See discussions, stats, and author profiles for this publication at: <https://www.researchgate.net/publication/258468263>

Constraining the kinetics of mantle phase changes with seismic data

Article in Geophysical Journal International · December 2011

DOI: 10.1111/j.1365-246X.2012.05417.x

CITATIONS

3

READS

30

4 authors, including:



Stephanie Durand

University of Münster

23 PUBLICATIONS **68** CITATIONS

[SEE PROFILE](#)



Jan Matas

Ecole normale supérieure de Lyon

37 PUBLICATIONS **715** CITATIONS

[SEE PROFILE](#)



Yanick Ricard

French National Centre for Scientific Research

183 PUBLICATIONS **6,257** CITATIONS

[SEE PROFILE](#)

Some of the authors of this publication are also working on these related projects:



Seisglob [View project](#)



The Earth's mantle transition zone [View project](#)

Constraining the kinetics of mantle phase changes with seismic data

S. Durand, F. Chambat, J. Matas and Y. Ricard

Laboratoire de Sciences de la Terre, CNRS UMR5570, École Normale Supérieure de Lyon, Université de Lyon, Université Claude Bernard Lyon 1, 46 Allée d'Italie, 69364 Lyon Cedex 07, France. E-mail: stephanie.durand@ens-lyon.fr

Accepted 2012 February 7. Received 2012 February 7; in original form 2011 June 14

SUMMARY

In a system where two phases coexist, a seismic wave can disrupt the pre-existing equilibrium and induce a re-equilibration process. Because the kinetics of the phase change is not instantaneous, the transformation induces an attenuation of the wave that can be quantified using an appropriate physical theory. Kinetics of Earth's phase transitions are not well known: in this paper we show that they can be constrained by seismic attenuation data. We quantify the influence of a phase transition upon seismic mode attenuation and body wave reflexion coefficient. We perform a numerical application for the olivine to wadsleyite transition at 410 km depth, assuming a phase loop thickness of 10 km. We show that the relaxation time that controls the frequency band of attenuation and the velocity at which the interface evolves when submitted to a pressure disequilibrium, is likely larger than 7000 s. For this kinetics slower than typical seismic waves periods, the transformation loop does not affect *S* waves attenuation but potentially that of *P* waves and normal modes.

Key words: Elasticity and anelasticity; Phase transitions; Body waves; Surface waves and free oscillations; Seismic attenuation; Wave propagation.

1 INTRODUCTION

Mantle material undergoes various phase changes that are induced by the increase of pressure with depth in Earth's interior. As these mineralogical transformations have finite kinetic times, they may dissipate the elastic energy carried by various seismic waves. Indeed, when an elastic wave propagates through a zone with a two-phase equilibrium, the associated stress oscillations disrupt the equilibrium and re-equilibration processes are activated. As the reaction is not infinitely fast, the re-equilibration does not instantaneously follow the perturbation induced by the wave. As a result, the wave undergoes attenuation and dispersion (see, e.g. de Groot & Mazur 1984, ch. XII, for a fluid–fluid phase change).

Vaisnys (1968) estimates that this anelastic mechanism may significantly contribute to the attenuation in the Earth's mantle in the case of solid–liquid phase transformations. The possible attenuation effects of solid–solid phase changes are considered by Tamisiea & Wahr (2002) who conclude that the impact of phase change kinetics may be important for normal modes. Li & Weidner (2008) and Weidner & Li (2010) experimentally study the low frequency compressibility associated with major mantle phase changes and propose that the resulting compressional attenuation may significantly affect seismic *P* and *S* waves. Ricard *et al.* (2009) show that a full viscoelastic model should be considered when modelling a solid–solid phase change and that it may induce both compressional and shear attenuation in two frequency bands, one of them being potentially in the range of normal seismic modes. This model has been challenged by Li (2010), who advocates for an attenuation band located at much higher frequency.

The dispersion and attenuation are usually quantified by a volumetric quality factor Q accounting for attenuation occurring within large depth intervals such as the whole lower mantle (see e.g. Dahlen & Tromp 1998, Section 9.7). This volumetric attenuation has been attributed to various mechanisms (stress induced motion of dislocations, thermoelastic relaxation, partial melting, the presence of fluid ...) (see e.g. Jacskon 2007, for a review). The interfacial contributions to attenuation, occurring within the narrow zones of coexisting mineralogical phases, have been neglected. The 1-D seismic models of attenuation are deduced from normal modes/surface wave or body wave attenuation measurements. Because shear losses are dominant, early studies attempted to explain attenuation data by shear attenuation Q_μ only (Anderson & Archambeau 1964; Kovach & Anderson 1964). However, these models do not acceptably fit the damping of radial modes: bulk attenuation Q_κ is required (Anderson & Hart 1978). Various depth-dependent Q_μ and Q_κ models have since been developed (Anderson 1980; Dziewonski & Anderson 1981; Durek & Ekström 1995, 1996; Resovsky *et al.* 2005). They only agree on some features: a low Q_μ in asthenosphere, an increase with depth of Q_μ and the necessity of a finite Q_κ (see reviews by Romanowicz & Durek 2000; Romanowicz & Mitchell 2007). Our knowledge of the radial structure of attenuation is limited by the weak sensitivity of normal modes to the lower mantle. Lawrence & Wyssession (2006) suggest to enhance the resolution of the 1-D models by using differential *S/ScS* amplitude measurements. The next step in improving our knowledge of attenuation should be to jointly inverse *S/ScS* differential amplitude measurements, normal mode attenuation data and to take into account the frequency dependence of Q (Lekic *et al.* 2009).

In this paper, we first apply the viscoelastic model for solid–solid transformation developed by Ricard *et al.* (2009) to quantify its effect on the attenuation of seismic modes as a function of the relevant physical parameters (phase change kinetics and thickness, elastic properties). The comparison of the predicted attenuation values with those observed for a selected mantle phase change provides constraints on its kinetic time. We also compute the reflexion coefficients of an *SH* wave with a normal incidence on an attenuating layer. We show that a careful analysis of these coefficients can bring additional constraints on the phase kinetics.

2 ATTENUATION IN A PHASE TRANSITION

Attenuation of sound in a liquid undergoing a phase change is a classical example of irreversible process that leads to attenuation (de Groot & Mazur 1984). The attenuation is expressed by a complex bulk modulus in the frequency domain, and more precisely it is found that the bulk modulus in such a liquid has a standard linear solid form:

$$\kappa(\omega) = \kappa_\infty + \frac{\kappa_0 - \kappa_\infty}{1 + i\omega\tau_0}, \quad (1)$$

where ω is the frequency of the sound wave, τ_0 is a characteristic time of the phase change, $\kappa_\infty = \kappa(\infty)$ is the bulk modulus at infinite frequency and $\kappa_0 = \kappa(0) \leq \kappa_\infty$ the bulk modulus at zero frequency. If the wave frequency is much larger than $1/\tau_0$ then the wave does not trigger a composition change: κ_∞ can be identified with the bulk modulus at constant composition and is often called the ‘unrelaxed’ bulk modulus. The unrelaxed compressibility, $1/\kappa_\infty$, is the average of the compressibilities of the coexisting phases weighed by their proportions. On the contrary, at very low frequency, the chemical reaction occurs at thermodynamic equilibrium and κ_0 is called the ‘relaxed’ bulk modulus. This modulus is simply the ratio of the pressure interval ΔP over which the transformation occurs to the relative density difference $\Delta\rho/\rho$ between the two phases: $\kappa_0 = \rho\Delta P/\Delta\rho$. In the two extreme cases ($\omega = 0$ or $\omega = \infty$), the bulk modulus is real which means that no dissipation occurs. In the intermediate regime, κ depends upon the frequency and has an imaginary part that yields attenuation. In seismology, the usual implicit hypothesis is that no reaction occurs and to identify κ_∞ with the bulk seismological modulus.

The model for attenuation of sound in a liquid is not sufficient for the purpose of seismology. First, the phase transformations in the mantle are not univariant but occur within a coexistence loop. For instance, the olivine to wadsleyite phase change at 410 km depth is about 10 km thick (Akaogi *et al.* 1989; Katsura & Ito 1989) and the garnet-to-perovskite transformation at 660 km about 50 km thick (Akaogi *et al.* 2002; Hirose 2002). Secondly, in a solid Earth material, shear deformation also attenuates the wave energy. Thirdly, because of the elastic shear stress, the bulk wave deformation is not entirely transmitted to the minor grains of the mineral aggregate. Thus, Ricard *et al.* (2009) made a simple thermomechanical model of the equilibrium loop of a divariant solid–solid phase transformation involving both bulk and shear deformations. They show that the resulting medium has a standard linear solid viscoelastic behaviour whose attenuation mainly depends upon the phase change kinetic rate. When no reaction occurs, the two phases have the same velocity measured on the grain interface, so $[v] = 0$ ($[v]$ is the jump in normal velocity on the interface). When the normal stress changes by $\delta\sigma_n$, Ricard *et al.* (2009) assumes that the interface moves with

a linear kinetics

$$[v] = C \delta\sigma_n = \frac{R_e}{\tau\kappa_\infty} \delta\sigma_n, \quad (2)$$

where the kinetic constant C is expressed as a function of R_e , a typical grain size, a typical high-frequency incompressibility κ_∞ and τ a kinetic time constant. They obtain that the bulk and shear moduli are given by

$$\kappa(\omega) = \kappa_\infty + \frac{\kappa_i - \kappa_\infty}{1 + i\omega\tau_\kappa}, \quad (3)$$

$$\mu(\omega) = \mu_\infty + \frac{\mu_i - \mu_\infty}{1 + i\omega\tau_\mu}. \quad (4)$$

In these equations, similar to eq. (1), τ_κ and τ_μ are the bulk and shear characteristic relaxation times [in Ricard *et al.* (2009), τ_κ and τ_μ were labelled τ_1 and τ_3 and were expressed in eqs (14) and (27)]. The elastic parameters κ_i and μ_i are the bulk and shear moduli at periods much longer than seismic periods but shorter than the mantle Maxwell time (see eqs (15), (25) and (26) for κ_i and μ_i in Ricard *et al.* 2009). Within a purely elastic matrix, the shear stresses never totally relax; they vanish only if the viscous relaxation is taken into account but this occurs on the much longer Maxwell time scale η/μ_∞ of a few thousand years (η is viscosity, which is likely a result of diffusion creep between grains). This is why there exist this ‘intermediate frequency’ moduli κ_i and μ_i that can be considered as relaxed with respect to the short time scale of seismic waves and can be seen as unrelaxed with respect to the large time scale of viscous flow. In other words, $\kappa_i = \kappa_0$ and $\mu_i = 0$ only if $\mu_\infty = 0$. These low frequency moduli, like the characteristic times τ_κ and τ_μ , vary slightly with the phase composition within the equilibrium loop (see Ricard *et al.* 2009, Fig. 2), but the second remain close to the time τ defined in eq. (2) with $\tau_\mu \approx 0.6\tau$ slightly larger than $\tau_\kappa \approx 0.4\tau$.

To illustrate the possible attenuation associated with a phase transformation, we consider the transition of olivine to wadsleyite, which is responsible for the major characteristics of the interface at the depth of 410 km. We choose this interface because it is believed to be a simple one where only one divariant phase transition occurs, a transition that does not need a large scale diffusion of elements and thus may occur relatively rapidly. A thickness of the transition between 5 and 10 km is often proposed from mineralogy or seismology (Akaogi *et al.* 1989; Katsura & Ito 1989; Shearer 2000; Ricard *et al.* 2005; Frost 2008) but some large values as 30 km have been reported (Van der Meijde *et al.* 2003). As Ricard *et al.* (2009), we will thus consider the intermediate case of a 10 km thickness.

Within the transition, in the model of Ricard *et al.* (2009), κ_i and μ_i depend on κ_0 , κ_∞ , μ_∞ and upon the volumic proportion ϕ of the two phases in the aggregate, but not on the kinetic constant C . Their evolution, assuming a linear variation of ϕ with the depth in the phase transition zone, is shown Fig. 1. τ_κ and τ_μ depend on κ_∞ , μ_∞ , ϕ and the kinetic constant τ . κ_0 , κ_∞ and μ_∞ are known from radial Earth models. Using PREM (Preliminary Reference Earth Model) values, yields $\kappa_\infty \approx 180$ GPa, $\kappa_0 \approx 7$ GPa, $\rho/\Delta\rho \approx 20$ and $\mu_\infty \approx 85$ GPa (see Fig. 1).

If the phase kinetic constant C were known with accuracy, it would be straightforward to predict the attenuation of body waves and seismic modes. However, available information on phase kinetics from laboratory experiments is limited (Kubo *et al.* 1998a,b; Liu *et al.* 1998; Mosenfelder *et al.* 2001; Li & Weidner 2008). Most laboratory measurements have been performed at temperatures up

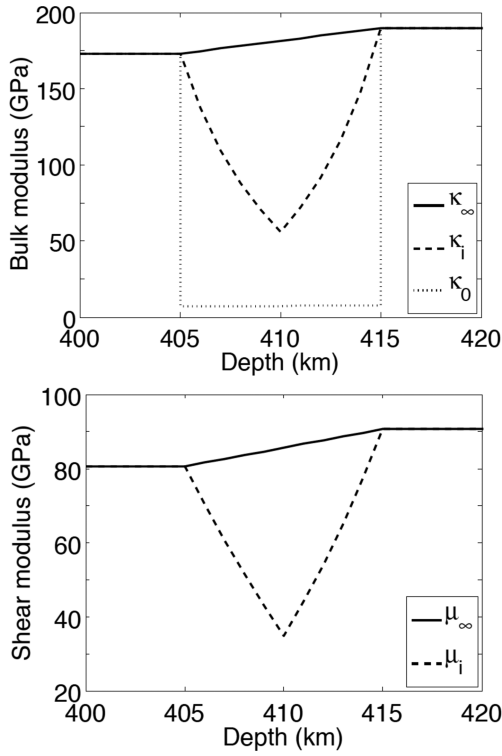


Figure 1. (Top panel) relaxed (κ_0), intermediate (κ_i) and unrelaxed (κ_∞) bulk moduli at the 410 km phase change. (Bottom panel) intermediate (μ_i) and unrelaxed (μ_∞) shear moduli at the 410 km phase change. Within the phase loop, the unrelaxed bulk and shear moduli are supposed to vary linearly between PREM values on the two sides of the transition.

to 400 K lower than the temperatures relevant to average mantle at 410 km and significant pressure overshoots have been imposed to activate the phase change (e.g. Mosenfelder *et al.* 2001). The experimental conditions (isothermal with small grain sizes) are also different from those in the mantle (adiabatic with likely larger grain sizes). Furthermore, minor components can significantly affect the phase kinetics, for example the presence of hydrogen protons can speed up the chemical diffusion by a factor of 50 (Hier-Majumder *et al.* 2005). All these experiments, however, suggest rapid kinetics with characteristic times comparable with seismic wave periods. In Sections 3 and 4, we constrain the relaxation time of the phase transition at 410 km depth using seismic observations. We come back to the implications of the seismic observations for the phase kinetics in the Discussion section.

3 INFLUENCE OF PHASE CHANGES UPON SEISMIC MODES

3.1 Mode attenuation

Seismic mode attenuation is usually estimated using a perturbation of a reference spherical non-attenuating model with real elastic parameters. According to Dahlen & Tromp (1998, eq. 9.54), the attenuation of a mode q (the inverse of its quality factor Q) can be expressed as a linear functional of the local attenuation:

$$q = \int_0^R (K_\kappa \delta_i \kappa + K_\mu \delta_i \mu) (r) dr, \quad (5)$$

where $K_\kappa(r)$ and $K_\mu(r)$ are respectively the compressional and shear

kernels, R the Earth's radius and $\delta_i \kappa$ and $\delta_i \mu$ the imaginary parts of the bulk and shear moduli.

The purpose of this section is to estimate the part in the mode attenuation that comes from the phase change zone only. If we express the imaginary part using eqs (3) and (4) and insert them into eq. (5), we see that the attenuation as a result of the phase change only is given by

$$q_{410} = \int_{r^-}^{r^+} \left(K_\kappa \frac{\kappa_\infty - \kappa_i}{1 + \omega^2 \tau_\kappa^2} \omega \tau_\kappa + K_\mu \frac{\mu_\infty - \mu_i}{1 + \omega^2 \tau_\mu^2} \omega \tau_\mu \right) (r) dr, \quad (6)$$

where r^- and r^+ are the lower and upper radii of the phase transition region.

In eq. (5), the kernels K_μ and K_κ are computed for a reference model. In our case, the reference model is also dependent on the period as the unrelaxed high frequency value κ_∞ and μ_∞ can be significantly different from the relaxed low frequency κ_i and μ_i (see Fig. 1). Thus, to minimize the perturbations we compute two sets of kernels using the program MINEOS. The unrelaxed reference model (i.e. PREM replaced near the transition by the thick lines of Fig. 1) is used when $\omega \tau > 1$, the relaxed model (i.e. PREM replaced near the transition by dashed lines of Fig. 1) when $\omega \tau < 1$. As the time constants do not vary much within the loop, we can replace with a good approximation eq. (6) by

$$q_{410} = \frac{\omega \tau_\kappa}{1 + \omega^2 \tau_\kappa^2} \int_{r^-}^{r^+} K_\kappa (\kappa_\infty - \kappa_i) dr + \frac{\omega \tau_\mu}{1 + \omega^2 \tau_\mu^2} \int_{r^-}^{r^+} K_\mu (\mu_\infty - \mu_i) dr, \quad (7)$$

where we use $\tau_\mu \approx 0.6 \tau$ and $\tau_\kappa \approx 0.4 \tau$.

The bulk and shear attenuations for the various modes are directly proportional to the kernels at the considered depth. Some examples of the compressional and shear kernels, computed with respect to the unrelaxed model, for radial modes ${}_0S_0$, ${}_1S_0$ and ${}_2S_0$ are shown in Fig. 2. These kernels do not cancel in the mantle transition zone and the mode attenuations are therefore affected by the phase changes occurring in this region.

3.2 Data set

Observations are provided by broad-band seismology that yields estimates of mode attenuations. The REM website gives measurements for 175 spheroidal and 73 toroidal seismic modes obtained by different authors (Li *et al.* 1991; Masters & Widmer 1995; Durek & Ekström 1996; He & Tromp 1996; Resovsky & Ritzwoller 1998; Masters, G., Laske G., Romanowicz, B. and Um, J., unpublished). When different q -values are given by several authors for the same mode, we average them. Two measurements are not included in the REM compilation, the modes ${}_0S_2$ and ${}_5S_{13}$, which we get from Masters & Widmer (1995). Taken together, spheroidal and toroidal data sets yield a total of 250 q -values shown in Fig. 3.

3.3 Constraints on the attenuation band

The values of q_{410} associated with the olivine to wadleyite phase change are computed for various modes using the values of κ_∞ , κ_i , μ_∞ and μ_i shown in Fig. 1 and considering an arbitrary kinetic time τ of 250 s. They are presented in Fig. 4 showing that the influence of the phase change upon mode attenuation is significant compared to the observed q_{obs} , particularly for spheroidal modes. The shape of the curves with the harmonic degree is related to compressibility and shear kernels.

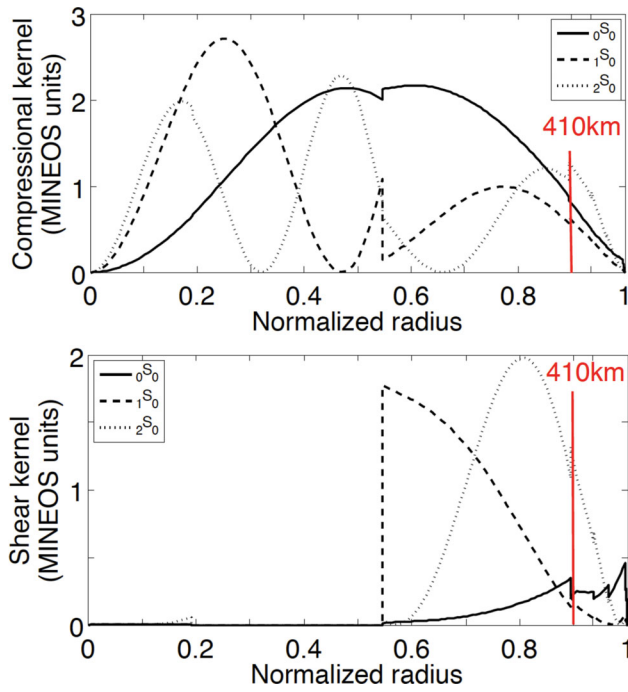


Figure 2. Compressional and shear kernels, $\kappa_{\infty}K_{\kappa}$ (top panel) and $\mu_{\infty}K_{\mu}$ (bottom panel), for the first three radial modes ${}_0S_0$, ${}_1S_0$ and ${}_2S_0$. The vertical bar indicates the position of the 410 km depth phase change. The reference model is unrelaxed (PREM modified for a linear gradient in the 410 km loop). The normalization is standard and explained in MINEOS.

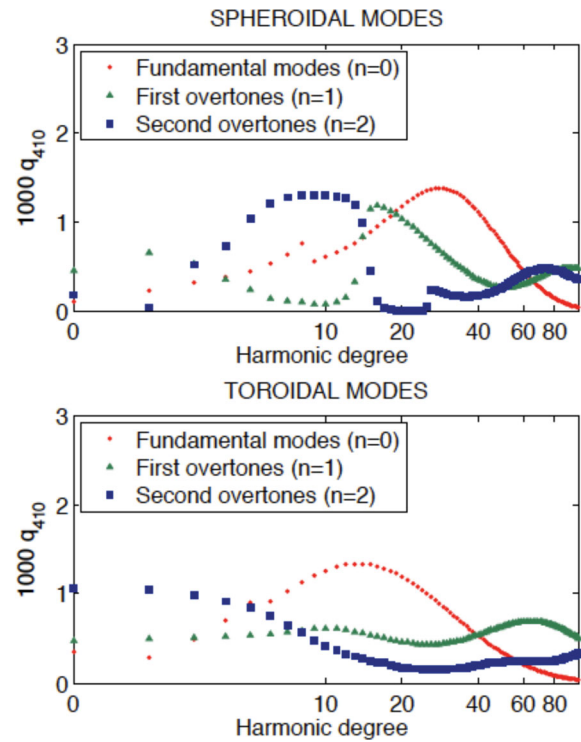


Figure 4. Calculated values of q_{410} for the first three branches ($n = 0, 1, 2$) of spheroidal (top panel) and toroidal (bottom panel) modes as a function of the harmonic degree. The attenuation are computed from eq. (7) for $\tau = 250$ s.

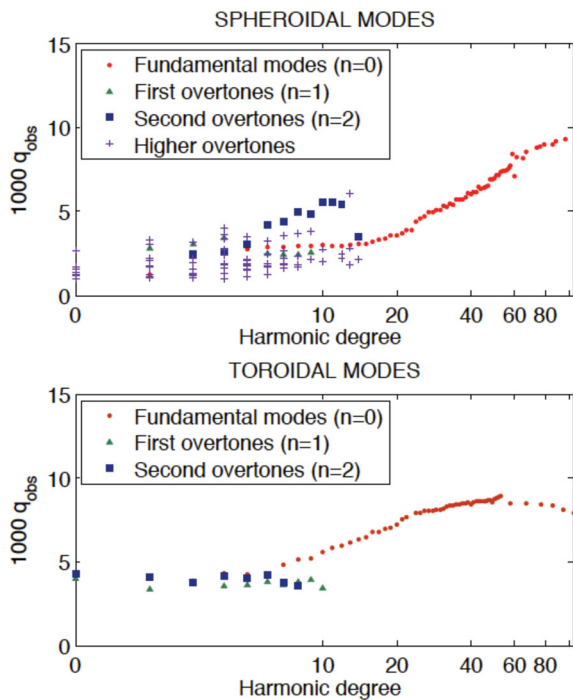


Figure 3. Observed attenuations for the 177 spheroidal (top panel) and 73 toroidal (bottom panel) modes as function of the harmonic degree. The possible attenuation because of phase changes must be lower than these observed values.

Fig. 5 shows the curve $q_{410}(\tau)/q_{\text{obs}}$ for various modes as a function of τ . When it is greater than 1, the contribution of the phase change alone is predicted to be larger than the observed value: this is impossible and excludes an interval of τ values. For instance, the observed attenuation of the mode ${}_0S_0$ implies that the reaction time of the olivine to wadsleyite reaction at mantle conditions is strictly slower than 387 s or strictly faster than 185 s. All together, upon the 250 measurements of q , 19 modes have their predicted q_{410} -values larger than that observed. In Fig. 6 the forbidden bands are detailed for each of the 19 modes labelled along the horizontal axis, that all together, exclude the periods shadowed on the graph. Therefore, to

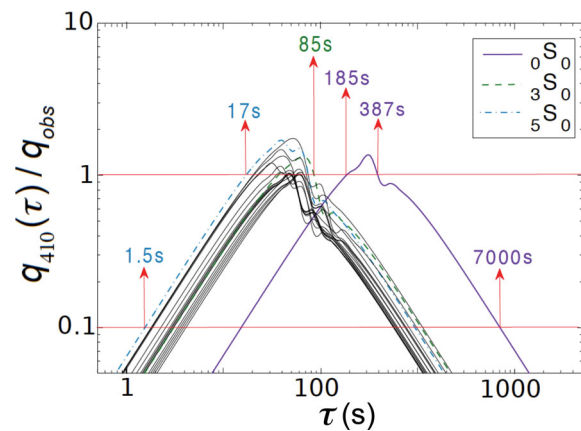


Figure 5. The 19 modes with $q_{410}(\tau)/q_{\text{obs}} > 1$. For instance, ${}_0S_0$ has a $q_{410}(\tau)/q_{\text{obs}} > 1$ for τ belonging to 185–387 s, so we must exclude this range of kinetic times. If we summarize all the constraints from all those 19 modes, we finally find that τ must be either below 17 s, between 85–185 s or above 387 s.

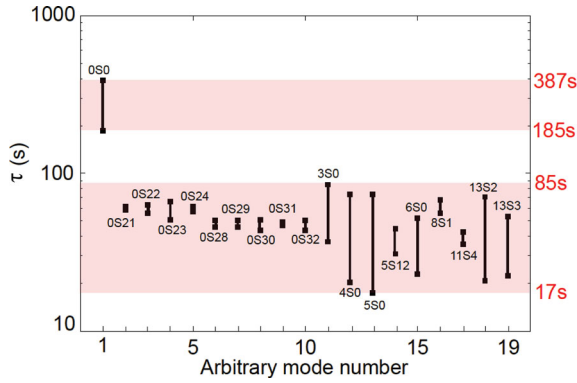


Figure 6. The 19 excluded ranges of kinetics in seconds as a function of an arbitrary mode number. Each mode is identified by its name. The real value of τ must be either below 17 s, between 85–185 s or above 387 s. Shaded areas indicate the excluded range of kinetics.

satisfy the observational constraints, the kinetic time τ must belong to $[0, 17] \cup [85, 185] \cup [387, +\infty]$ s. Mode ${}_0S_0$ forbids the $[185, 387]$ s range, although mostly ${}_3S_0$ and ${}_5S_0$ forbid the $[17, 85]$ s range.

Inferring the consequences of $q_{410}(\tau)/q_{\text{obs}} \leq 1$ does not mean that this bound can be reached. Indeed, observed mode attenuations cannot be explained entirely by the 410 km phase transition as volumetric attenuation occurs elsewhere into the Earth. To refine the constraints on τ , one would wish to subtract the known volumetric attenuation to q_{obs} . This cannot be done rigorously. However, as PREM or QL6 (Durek & Ekström 1996) already explain the attenuation of the modes within 12 and 11 per cent and as various phase transitions could be considered (at least that at 670 km depth), we can reasonably consider that the 410 km depth phase transition can hardly contribute to the mode attenuation by more than 10 per cent. The corresponding bound, $q_{410}(\tau)/q_{\text{obs}} \leq 0.1$, implies that all kinetics times τ must belong to $[0, 1.5] \cup [7000, +\infty]$ s (as seen in Fig. 5). Eqs (5)–(7) are obtained by linearly perturbing an elastic model. We check *a posteriori* that this approximation is valid: for $\tau < 1.5$ s or $\tau > 7000$ s the relative perturbations of the elastic parameters in the coexistence loop are less than 0.1 per cent.

4 INFLUENCE OF PHASE CHANGES UPON REFLEXION COEFFICIENTS

The normal modes impose either very fast or very slow kinetic times. We now try to put more constraints on the exclusion range by considering the effect of phase transition on body waves. Indeed, if the kinetic time is shorter than or within the range of body wave periods, body waves crossing the phase loop will experience partially relaxed elastic moduli and a strong attenuation that will affect their propagation and therefore the reflectivity of the 410 km depth discontinuity. We are, therefore, going to compare the observed and computed normal incidence reflexion coefficients of an S wave crossing the phase transition.

4.1 Reflectivity measurements

Revenaugh & Jordan (1991) estimate the normal incidence reflectivity of the 410 km discontinuity by inverting the amplitude of the ScS_n and $sScS_n$ core-reflections phases for short epicentral distances and periods of 40 s in South West Pacific. They found a reflection coefficient at 410 km of about 5 per cent. Another study by Revenaugh & Sipkin (1994) uses the same kind of data but under

China, and reports reflection coefficients varying from 3 to 6 per cent for periods of 25 s. The horizontal component of the SS precursors that under-reflect on the 410 km discontinuity, denoted $S410S$, can also constrain the normal incidence reflectivity of the discontinuity. These phases have been used by Chambers *et al.* (2005) who find a reflection coefficient for periods of 15–75 s of about 4.4 ± 1.4 per cent. We will, thus take as an observational constraint a reflection coefficient of 3 to 6 per cent for incidence close to normal and for periods ranging from 20 to 40 s.

4.2 Body wave reflection coefficient in a layer undergoing a phase change

We perform the computation of the reflexion coefficients of a loop layer having exactly the complex rheological laws of eqs (3) and (4), embedded between two elastic half-spaces. The elastic waves are propagated using the Thomson–Haskell matrixial propagator method (Haskell 1953; Kennett 2009). The layer is divided into n sublayers to take into account the evolution of κ_i , μ_i (see Fig. 1) and of the density (linearly varying through the loop). In each sublayer the motion equation is solved and the continuity of displacement and stress is applied at each interface. It yields the reflexion and transmission coefficients, function of the wave frequency and of the phase kinetic time. The reflexion coefficient is shown for a downgoing wave, normal to the interface (Fig. 7), and is very similar for an upgoing wave.

4.3 Constraints on the kinetics

Fig. 7 shows the reflexion coefficient of the interface as a function of the kinetic time τ and the wave period. Constructive and destructive interferences of the multireflected waves lead to oscillations of the reflexion coefficients when the period of the seismic wave approaches zero (Lees *et al.* 1983). For the typical period that have been used for seismic observations (20–40 s), the transitional kinetic time for which the loop properties change from relaxed to unrelaxed is around $\tau = 5$ s. For a slow kinetics of the phase transition, $\tau \gg 5$ s, the wave propagates in a PREM-like model and the reflexion coefficient is typically of order 3 per cent. For a fast kinetics, $\tau \ll 5$ s, the phase loop behaves as a low velocity layer which traps the incident wave and the computed reflexion coefficient is

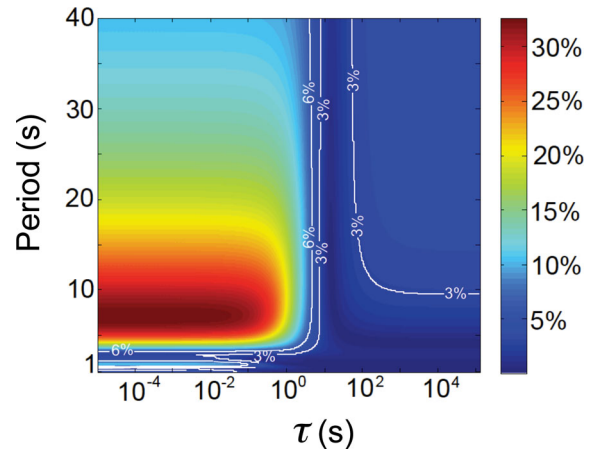


Figure 7. Reflexion coefficient of a vertically propagating SH wave through a 10 km thick attenuative layer which undergoes the phase change olivine-to-wadsleyite, as a function of phase reaction time τ and wave period. For typical 20–40 s periods, the phase loop is an unrelaxed layer for $\tau \gg 5$ s, whereas for $\tau \ll 5$ s it appears as a relaxed (and low velocity) layer.

much higher than what is observed. Examining Fig. 7 and taking into account the constraints from the observations that the reflexion coefficient is between 3 and 6 per cent for periods ranging from 20 to 40 s, we can deduce that the body wave observations impose a kinetic time either in $[5, 8] \cup [63, +\infty]$ s.

5 DISCUSSION

We have designed a method to quantify the contribution to attenuation resulting from regions with coexisting phases using seismic modes and body wave reflexion coefficients. An example with the transition at 410 km shows that the effect is not negligible and strongly depends on the characteristic time τ of the phase change. Comparing observations and our numerical predictions, normal mode attenuation data and body wave reflection coefficients can thus constrain τ ; in the case of a 10 km thick olivine to wadsleyite phase change we find that τ must strictly belong to $[5, 8] \cup [85, 185] \cup [387, +\infty]$ s. If we consider, more realistically that at most 10 per cent of the attenuation can be related to this specific attenuation mechanism, only the interval $[7000, +\infty]$ s is allowed (Fig. 8). Our

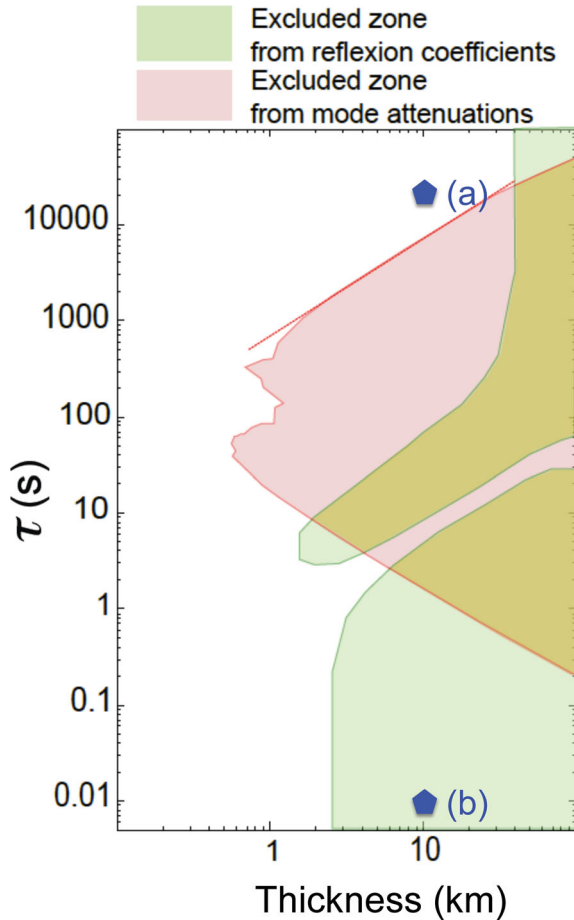


Figure 8. Excluded range (coloured shades) of kinetics as a function of the transition thickness with the parameters of PREM at 410 km depth and considering $q_{410} < 0.1 q_{\text{obs}}$. For a thickness smaller than 600 m, no mode attenuation or body wave reflectivity data constrains the kinetics of the transition. The condition $\tau(s) > 700 h(\text{km})$ (dotted red line) summarizes the likely zone of the kinetic time. The two blue points are kinetic times deduced from mineralogical experiments: (a) Kubo *et al.* (1998a) and (b) Li & Weidner (2008).

approach has enabled us to identify the kinetics that are in contradiction with seismic observations and therefore that must be excluded. This does not imply that accounting for interface attenuation in 1-D seismological model would necessarily significantly improve the fit with observations of Earth's attenuation. However, this suggests that interfacial attenuation should be considered in seismological models.

A noteworthy consequence of the phase change is that it yields a shear as well as a bulk attenuation. Because bulk attenuation is on average small outside phase changes, compressional modes provide a strong constraint on the phase kinetics: as shown by Fig. 6, the exclusion intervals are provided by modes ${}_0S_0$, ${}_3S_0$ and ${}_5S_0$. Because of the shape of mode kernels, most of the attenuation of these spheroidal modes is a result of bulk relaxation.

The thickness of the phase change is a parameter that affects the results and is poorly known. The evolution of the forbidden bands as function of this thickness is depicted in Fig. 8 (coloured shades). For a thickness of 10 km, we recover the possible intervals that we discussed before: $[0, 1.5] \cup [7000, +\infty]$ s for the modes and $[5, 8] \cup [63, +\infty]$ s for the body waves, which together impose $\tau > 7000$ s. The properties of a very thin transition zone do not affect much the attenuation of modes (below 600 m thick) and the reflexion coefficients (below 2–3 km thick) and are therefore invisible to seismic observations. However, such a thin transition zone would be in contradiction with mineralogical and seismological data (e.g. Katsura & Ito 1989; Shearer 2000). For a larger thickness, the exclusion band is controlled at low frequency by seismic modes (assuming $q_{410} < 0.1 q_{\text{obs}}$) until a thickness of 40 km. In the range of thicknesses of 1–40 km, the kinetic time τ must be larger than a minimum time τ_{min} increasing linearly with the transition thickness, h , and thus of order $\tau_{\text{min}}(\text{s}) \approx 700 h(\text{km})$ (dotted red line on Fig. 8). The reflexion coefficient forbids the too short kinetic times. Above 40 km, Fig. 8 shows that the predicted mode attenuations or reflexion coefficients are always in contradiction with the seismic data. Because for such a large transition the reflexion coefficients become too small, the maximum thickness allowed for the olivine to wadsleyite phase change is thus 40 km.

The bulk attenuation within the transformation loop is given by:

$$q_{\kappa} = \frac{(\kappa_{\infty} - \kappa_i) \omega \tau_{\kappa}}{\kappa_i + \omega^2 \tau_{\kappa}^2 \kappa_{\infty}}. \quad (8)$$

The limit $\tau = 7000$ s is larger than body waves and normal modes periods ($\omega \tau \gg 1$) and imposes a maximum value for the attenuation in the loop $q_{\kappa} < (\kappa_{\infty} - \kappa_i) / (\omega \tau_{\kappa} \kappa_{\infty})$. Similar expressions hold for q_{μ} . These limits are depicted in Fig. 9 (considering mean values in the loop $\kappa_i \approx 100$ GPa, $\mu_i \approx 50$ GPa) and compared with upper-mantle PREM values. It shows that the shear attenuation q_{μ} of body waves within the transformation loop (solid red line) is less than that of the upper mantle (dashed red line): the transformation loop should not affect the S -wave attenuation. On the contrary, P -wave attenuation is potentially affected by the transformation loop. For normal modes, the transformation potentially affects q_{κ} and also q_{μ} . However, the fact that the phase transformation can affect seismic attenuation in a 10 km thick layer does not imply that seismic 1-D models have yet enough depth resolution to identify this layer.

Morris (2002) writes $V = c \delta \sigma_n$, where V is the interface velocity. His definition is not appropriate for our model in which compressibility allows the motion of the interface even without phase change. We, therefore, use $[v] = C \delta \sigma_n$ [see eq. (2)], however, as the interface velocity is rather a result of phase change than of compressibility, $C \approx (\Delta \rho / \rho) c$. Using experimental values on olivine–wadsleyite transformation for 1 mm grain size and the low temperature of

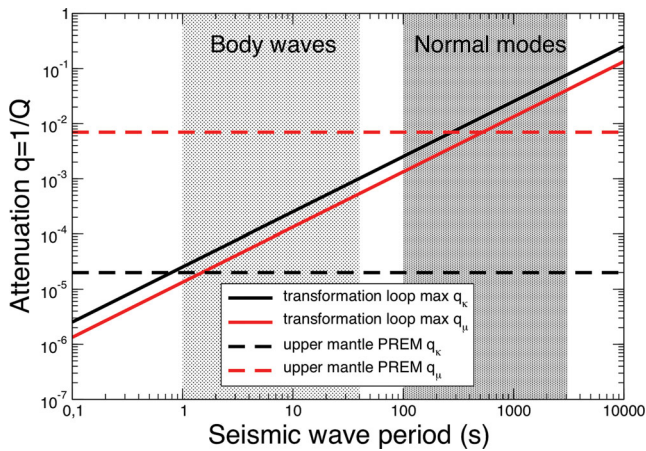


Figure 9. Maximum values for q_k (solid black line) and q_μ (solid red line) imposed by the constraint $\tau > 7000$ s in the transformation loop. PREM upper-mantle values are shown by dashed lines. The typical period ranges of body waves and normal modes are shaded. The transformation loop does not affect S waves attenuation but potentially that of P waves and normal modes.

1300 K, [$c = 45 \text{ nm s}^{-1} \text{ GPa}^{-1}$, $C = 2.25 \text{ nm s}^{-1} \text{ GPa}^{-1}$ (Kubo *et al.* 1998a; Morris 2002)], we predict $\tau = 25\,000$ s for a grain size of 1 cm (note that in Ricard *et al.* (2009), we wrongly identify the measured c with our C , and 1250 s would have been found for the same grain size). This kinetic time is shown in Fig. 8 [blue point (a)] and is compatible with the seismically deduced constraint $\tau > 7000$ s and this is true as soon as the grain size is larger than 2.5 mm in the transition loop. The value predicted by Li & Weidner (2008), $\tau = 0.01$ s is also plotted [blue point (b)]. Their reaction rate measured for the olivine–ringwoodite transition lies in the exclusion zone and is significantly faster than the seismically deduced constraints for all reasonable grain sizes. However, we do not understand how the data are extrapolated from the laboratory to the real Earth by Li & Weidner (2008) and Li (2010). These authors themselves consider that, driven by an excess pressure of 1 GPa near the middle of the loop, the grain interfaces move by $2 \mu\text{m}$ within a characteristic time of 4000 s (see e.g. Li & Weidner 2008, fig. 2). A typical interface velocity that can be deduced from their experiments, $c = 0.5 \text{ nm s}^{-1} \text{ GPa}^{-1}$ is significantly slower than that deduced from Kubo *et al.* (1998a) and should lead to an attenuation band at much longer period.

The kinetic time τ that we deduce is only based on seismological data. Its relation to the phase kinetics parameter C assumes linearity between interface velocity and pressure perturbation. Such linear relation may be a result of an intrinsic finite rate of return to thermodynamic equilibrium or to other kinetic effects. Indeed, even at thermodynamic equilibrium, thermal diffusion of latent heat or chemical diffusion of elements both impose a linear relation between interface velocity and pressure perturbation (Loper & Fearn 1983; Tamisiea & Wahr 2002).

This constraint can also be applied to estimate a typical undulation of the 410 km interface, δz , because of the metastability of olivine. For a vertical velocity v_z and using eq. (2) with the stationarity condition $v = v_z$, it is possible to express δz :

$$\delta z = \frac{v_z \tau \kappa_\infty}{R_e \rho g}, \quad (9)$$

where ρ is the density and g the gravity. Using $v_z = 1 \text{ cm yr}^{-1}$, $\rho = 3600 \text{ kg m}^{-3}$, $g = 10 \text{ m s}^{-2}$ and $\tau = 7000$ s, it yields a distance of

about 10 km. This estimate is valid for a normal mantle temperature, in cold subducting slabs the kinetics would be much slower and the metastable wedge would reach much larger depth (Kirby *et al.* 1996; Mosenfelder *et al.* 2001).

ACKNOWLEDGMENTS

We thank Bernard Valette and Thierry Alboussière for stimulating discussions. This work has been supported by the french CNRS-INSU *SEDIT* and the ANR *Seisglob* (ANR 2011 Blanc SIMI 5-6 016 01).

REFERENCES

- Akaogi, M., Ito, E. & Navrotsky, A., 1989. Garnet-ilmenite-perovskite transitions in the system $\text{Mg}_4\text{Si}_4\text{O}_{12}\text{-Mg}_3\text{Al}_2\text{Si}_3\text{O}_{12}$ at high pressures and high temperatures: phase equilibria, calorimetry and implications for mantle structure, *Phys. Earth planet. Inter.*, **132**, 303–324.
- Akaogi, M., Tanaka, A. & Ito, E., 2002. Olivine-modified spinel-spinel transitions in the system $\text{Mg}_2\text{SiO}_4\text{-Fe}_2\text{SiO}_4$: calorimetric measurements, thermochemical calculation, and geophysical application, *J. geophys. Res.*, **107**, 15 671–15 685.
- Anderson, D.L., 1980. Bulk attenuation in the Earth and viscosity of the core, *Nature*, **285**, 204–207.
- Anderson, D.L. & Archambeau, C.B., 1964. The anelasticity of the Earth, *J. geophys. Res.*, **69**(10), 2071–2084.
- Anderson, D.L. & Hart, R.S., 1978. Q of the Earth, *J. geophys. Res.*, **83**, 5869–5882.
- Chambers, K., Deuss, A. & Woodhouse, J.H., 2005. Reflectivity of the 410-km discontinuity from PP and SS precursors, *J. geophys. Res.*, **110**, 2–13.
- Dahlen, F.A. & Tromp, J., 1998. *Theoretical Global Seismology*, Princeton University Press, Princeton, NJ, 1025pp.
- de Groot, S.R. & Mazur, P., 1984. *Non-Equilibrium Thermodynamics*, Dover Publications, New York, NY.
- Durek, J.J. & Ekström, G., 1995. Evidence of bulk attenuation in the asthenosphere from recordings of the Bolivia earthquake, *J. geophys. Res.*, **100**, 2309–2312.
- Durek, J.J. & Ekström, G., 1996. A radial model of anelasticity consistent with long-period surface wave attenuation, *Bull. seism. Soc. Am.*, **86**, 144–158.
- Dziewonski, A.M. & Anderson, D.L., 1981. Preliminary reference Earth model, *Phys. Earth planet. Inter.*, **25**, 297–236.
- Frost, D.J., 2008. The upper mantle and transition zone, *Elements*, **4**(3), 171–176, doi:10.2113/GSELEMENTS.4.3.171.
- Haskell, N.A., 1953. Dispersion of surface waves on multilayered media, *Bull. seism. Soc. Am.*, **43**, 17–34.
- He, X. & Tromp, J., 1996. Normal-mode constraints on the structure of the mantle and core, *J. geophys. Res.*, **101**, 20 053–20 082.
- Hier-Majumder, S., Anderson, I.M. & Kohlstedt, D.L., 2005. Influence of protons on Fe-Mg interdiffusion in olivine, *J. geophys. Res.*, **110**, doi:10.1029/2004JB003292.
- Hirose, K., 2002. Phase transitions in pyrolytic mantle around 670-km depth: implications for upwelling of plumes from the lower mantle, *J. geophys. Res.*, **107**, doi:10.1029/2001JB000597.
- Jackson, I., 2007. Properties of rocks and minerals—physical origins of anelasticity and attenuation in rock, in *Treatise on Geophysics*, Vol. 2, pp. 493–525, ed. Price, G.D., Elsevier, Amsterdam.
- Katsura, T. & Ito, E., 1989. The system $\text{Mg}_2\text{SiO}_4\text{-Fe}_2\text{SiO}_4$ at high pressures and temperatures: precise determination of stabilities of olivine, modified spinel-spinel, *J. geophys. Res.*, **94**, 15 663–15 670.
- Kennett, B.L.N., 2009. *Seismic Wave Propagation in Stratified Media*, Australian National University Electronic Press, Canberra.
- Kirby, H., Stein, S., Okal, E.A. & Rubie, D.C., 1996. Metastable mantle phase transformations and deep earthquakes in subducting oceanic lithosphere, *Rev. Geophys.*, **306**, 34–261.
- Kovach, R.L. & Anderson D.A., 1964. Attenuation of shear waves in the upper and lower mantle, *Bull. seism. Soc. Am.*, **54**, 1855–1864.

- Kubo, T., Ohtani, E., Kato, T., Shinmei, T. & Fujino, K., 1998a. Effects of water on the $\alpha - \beta$ transformation kinetics in San Carlos olivine, *Sciences*, **281**, 85–87.
- Kubo, T., Ohtani, E., Kato, T., Shinmei, T. & Fujino, K., 1998b. Experimental investigation of the $\alpha - \beta$ transformation of San Carlos olivine single crystal, *Phys. Chem. Miner.*, **26**, 1–6.
- Lawrence, J.F. & Wysession, M.E., 2006. QLM9: a new radial quality factor ($Q\mu$) model for the lower mantle, *Earth planet. Sci. Lett.*, **241**, 962–971.
- Lees, A.C., Bukowinski, M.S.T. & Jeanloz, R., 1983. Reflection properties of phase transition and compressional change models of the 670-km discontinuity, *J. geophys. Res.*, **88**, 8145–8159.
- Lekic, V., Matas, J., Panning, M. & Romanowicz, B., 2009. Measurement and implications of frequency dependence of attenuation, *Earth planet. Sci. Lett.*, **282**, 285–293.
- Li, L., 2010. Bulk attenuation in the Earth's mantle due to phase transitions, *Phys. Earth planet. Inter.*, **183**, 473–477. doi:10.1016/j.pepi.2010.09.012.
- Li, L. & Weidner, D.J., 2008. Effect of phase transitions on compressional-wave velocities in the Earth's mantle, *Nature*, **454**, doi:10.1038/nature07230.
- Li, X.-D., Giardini, D. & Woodhouse, J.H., 1991. Large-scale three-dimensional even-degree structure of the Earth from splitting of long-period normal modes, *J. geophys. Res.*, **96**, 551–577.
- Liu, M., Kerschhofer, L., Mosenfelder, J.L. & Rubie, D.C., 1998. The effect of strain energy on growth rates during the olivine-spinel transformation and implications for olivine metastability in subducting slabs, *J. geophys. Res.*, **103**, 23 897–23 909.
- Loper D.E. & Fearn D.R., 1983. A seismic model of partially molten inner core, *J. geophys. Res.*, **88**, 1235–1242.
- Masters, T.G. & Widmer, R., 1995. Free oscillations: frequencies and attenuations, in *Global Earth Physics, A Handbook of Physical Constants*, pp. 104–125, ed. Ahrens, T.J., American Geophysical Union, Washington, DC.
- Morris, S.J.S., 2002. Coupling of interface kinetics and transformation-induced strain during pressure-induced solid-solid phase changes, *J. Mech. Phys. Solids*, **50**, 1363–1395.
- Mosenfelder, J.L., Marton, F.C., Ross C.R., II, Kerschhofer, L. & Rubie, D.C., 2001. Experimental constraints on the depth of olivine metastability in subducting lithosphere, *Phys. Earth planet. Inter.*, **127**, 165–180.
- Resovsky, J.S. & Ritzwoller, M.H., 1998. New and refined constraints on 3-D Earth structure from normal modes below 3 mHz, *J. geophys. Res.*, **103**, 783–810.
- Resovsky, J.S., Trampert, J. & Van der Hilst, R.D., 2005. Error bars for the global seismic Q profile, *Earth planet. Sci. Lett.*, **230**, 413–423.
- Revenaugh, J. & Jordan, T., 1991. Mantle layering from ScS reverberations, 2. The transition zone, *J. geophys. Res.*, **96**, 19 763–19 780.
- Revenaugh, J. & Sipkin, S.A., 1994. Mantle discontinuity structure beneath China, *J. geophys. Res.*, **99**, 21 911–21 927.
- Ricard, Y., Mattern, E. & Matas, J., 2005. Synthetic tomographic images of slabs from mineral physics, in *Composition, Structure and Evolution of the Earth Mantle*, AGU Monograph Vol. 160, pp. 283–300, eds Hilst, R., Bass, J.D., Matas, J. & Trampert, J., American Geophysical Union, Washington, DC.
- Ricard, Y., Matas, J. & Chambat, F., 2009. Seismic attenuation in a phase change coexistence loop, *Phys. Earth planet. Inter.*, **176**, doi:10.1016/j.pepi.2009.04.007.
- Romanowicz, B. & Durek, J., 2000. Seismological constraints on attenuation in the earth: a review, in *Earth's Deep Interior: Mineral Physics, and Tomography from the Atomic to the Global Scale*, AGU Monograph Vol. 117, pp. 161–180, eds Karato, S., Forte, A.M., Liebermann, R.C., Masters, G. & Stixrude, L., American Geophysical Union, Washington, DC.
- Romanowicz, B. & Mitchell, B., 2007. Q of the Earth from crust to core, in *Treatise of Geophysics*, Vol. 1, pp. 731–774, eds Romanowicz, B. & Dziewonski, A., Elsevier.
- Shearer, P.M., 2000. Upper mantle seismic discontinuities, in *Earth's Deep Interior: Mineral Physics and Tomography from the Atomic to the Global Scale*, AGU Monograph, Vol. 117, pp. 115–131, eds Karato, S., Forte, A.M., Liebermann, R.C., Masters, G. & Stixrude, L., American Geophysical Union, Washington, DC.
- Tamisiea, M.E. & Wahr, J.M., 2002. Phase transitions and short timescale sinusoidal motions, *Phys. Earth planet. Inter.*, **198**, 459–470.
- Vaisnys, J.R., 1968. Propagation of acoustic waves through a system undergoing phase transformations, *J. geophys. Res.*, **73**, 7675–7683.
- Van der Meijde, M., Marone, F., Giardini, D. & van der Lee, S., 2003. Seismic evidence for water deep in Earth's upper mantle, *Science*, **300**, doi:10.1126/science.1083636.
- Weidner, D.J. & Li, L., 2010. Impact of phase transitions on P wave velocities, *Phys. Earth planet. Inter.*, **180**, 189–194, doi:10.1016/j.pepi.2009.11.006.